# A de novo missense mutation of human cardiac $Na^+$ channel exhibiting novel molecular mechanisms of long QT syndrome

Naomasa Makita[a,*], Nobumasa Shirai[a], Masato Nagashima[b], Rumiko Matsuoka[c], Yoichi Yamada[b], Noritsugu Tohse[b], Akira Kitabatake[a]

[a] *Department of Cardiovascular Medicine, Hokkaido University School of Medicine, Kita-15 Nishi-7, Kita-Ku, Sapporo 060-0815, Japan*
[b] *Department of Physiology, Sapporo Medical University, Sapporo 060-8556, Japan*
[c] *Department of Pediatric Cardiology, The Heart Institute of Japan, Tokyo Women's Medical College, Tokyo 162-0054, Japan*

Received 18 December 1997; revised version received 5 January 1998

**Abstract Mutations in a human cardiac $Na^+$ channel gene (SCN5A) are responsible for chromosome 3-linked congenital long QT syndrome (LQT3). Here we characterized a de novo missense mutation (R1623Q, S4 segment of domain 4) identified in an infant Japanese girl with a severe form of LQT3. When expressed in oocytes, mutant $Na^+$ channels exhibited only minor abnormalities in channel activation, but in contrast to three previously characterized LQT3 mutations, had significantly delayed macroscopic inactivation. Single channel analysis revealed that R1623Q channels have significantly prolonged open times with bursting behavior, suggesting a novel mechanism of pathophysiology in $Na^+$ channel-linked long QT syndrome.**



*Key words:* Long QT syndrome; Sodium channel; Voltage sensor; Inactivation; De novo mutation

## 1. Introduction

Congenital long QT syndrome (LQTS) is an inherited disorder characterized by prolonged ventricular repolarization and a predisposition for development of potentially lethal ventricular arrhythmias. LQTS is genetically heterogeneous with at least five distinct loci [1–5]. One locus (LQT3) on human chromosome 3p21 encodes the cardiac voltage-gated $Na^+$ channel α subunit (hH1) [2,6]. At present, three mutations in SCN5A have been identified; one in-frame deletion mutation of residues 1505–1507 (ΔKPQ) and two missense mutations (N1325S, R1644H) [2,7] (Fig. 1). Heterologously expressed mutant channels display macroscopic $Na^+$ currents with decay rates comparable to wild type (WT) hH1 but exhibit small persistent inward currents resulting from channel reopening during the late phase of a depolarizing stimulus [8–10].

In this study, we characterized a novel de novo SCN5A missense mutation [11], discovered in a female infant with an unusually severe form of LQT. The mutation results in the substitution of glutamine for arginine-1623 (designated R1623Q) located at the outermost positively charged residue of the S4 segment of domain 4 (S4/D4, Fig. 1), a putative voltage sensor of the $Na^+$ channel. When expressed heterologously, R1623Q exhibited persistent inward current as observed in previously characterized LQT3 mutations [8,9], however, its macroscopic inactivation rate was significantly slower than either the WT channel or other LQT3 mutations, demonstrating distinct pathophysiological mechanisms underlying this mutation.

## 2. Materials and methods

### 2.1. Construction of R1623Q mutant $Na^+$ channel

Amino acid substitution of glutamine for arginine-1623 (R1623Q) of human cardiac $Na^+$ channel α subunit (hH1) was performed by an overlap extension PCR strategy [12]. A 459 bp cDNA of hH1 was amplified using oligonucleotide primers hH1-4418F (5′-TCAACCAACAGAAAAAGT-3′) and R1623Q-R (5′-GGATGACTTGGAAGAGCGTCGG-3′). Similarly, a 165 bp cDNA of hH1 was amplified using oligonucleotide primers R1623Q-F (5′-CTCTTCCAAGTCATCCGCCTG-3′) and hH1-5006R (5′-GCCAAAGATGGAGTAGATGA-3′). Subsequently, the two PCR products were purified and combined in a second round of PCR with the primer pair hH-4418F and hH1-5006R. A 608 bp PCR product was digested with *Bam*HI/*Bst*EII and subcloned back into WT-hH1 to assemble the R1623Q-hH1 construct. Multiple independent clones were isolated and their sequence was verified by dideoxynucleotide sequencing of the final constructs.

### 2.2. RNA transcription and oocyte injection

WT-hH1 and R1623Q-hH1 engineered in the oocyte expression vector pSP64T [13] were used for in vitro transcriptions. Sense cRNAs were transcribed in vitro from *Xba*I linearized cDNAs using SP6 Cap scribe kit (Boehringer). Defolliculated *Xenopus* oocytes (stage V–VI) were injected with 40 nl (4–20 ng) of 5′-capped cRNAs encoding $Na^+$ channels and then incubated at room temperature in ND-96 solution (96 mM NaCl, 2 mM KCl, 1.8 mM $CaCl_2$, 1 mM $MgCl_2$, 5 mM HEPES (pH 7.50 with NaOH)) for 1–2 days [14,15].

### 2.3. Electrophysiology and data analysis

Whole-cell currents were recorded in oocytes using two-microelectrode voltage-clamp as previously described [15]. Electrodes were filled with 3 M KCl/1% agarose and then back filled with 3 M KCl to give low tip resistance (0.2–0.5 MΩ) [16]. Currents were filtered at 5 kHz (−3 dB; 4-pole Bessel filter) and data collection and analysis were performed using pClamp 6 (Axon Instruments). In some experiments, oocytes were perfused with ND-96 containing 30 μM tetrodotoxin (TTX, Sigma) to block $Na^+$ currents and allow determination of TTX-sensitive current components [8].

Inside-out patch-clamp recordings were performed as previously described [17] using a CEZ-2300 patch-clamp amplifier (Nihon Kohden, Japan). The patch pipettes had tip resistances of 5–10 MΩ and the pipette solution contained 145 mM NaCl, 1 mM $CaCl_2$, 2 mM $MgCl_2$, 10 mM HEPES (pH 7.35). Data were stored on digital audio tapes using a DAT data recorder. Current signals were filtered at 2 kHz (4-pole Bessel low-pass filter), digitized at 10 kHz and analyzed on a personal computer having an AD converter (ADX-98E, Canoopus Electronics, Japan). During single channel recording, oocytes were perfused with an external solution (110 mM CsF, 10 mM NaF, 20 mM CsCl, 2 mM EGTA, 10 mM HEPES (pH 7.35)). Under these conditions, K channel current is eliminated in the inside-out patch-clamp mode.

The time course of macroscopic current decay during a voltage step was fit with double-exponential functions: $I(t)/I_{max} = A_f \times \exp(-t/\tau_f) + A_s \times \exp(-t/\tau_s) + A_0$ ($t = 0$–40 ms), where $A_0$ is a constant value,

*Corresponding author. Fax: (81) (11) 706-7874.
E-mail: makitan@med.hokudai.ac.jp


*PII* S0014-5793(98)00033-7

$A_f$ and $A_s$ are fractions of fast and slow inactivating components, while $\tau_f$ and $\tau_s$ are the time constants of fast and slow inactivating components, respectively. Steady-state inactivation data were fit with the Boltzmann equation, $I/I_{max} = [1+\exp((V-V_{1/2})/k)]^{-1}$ to determine the membrane potential for half-maximal inactivation ($V_{1/2}$) and the slope factor $k$. Recovery from inactivation was analyzed by fitting data with a two-exponential equation using a non-linear least squares minimization method. Recovery rate $= A_f \times \exp(-t/\tau_f) + A_s \times \exp(-t/\tau_s) + A_0$, where $A_0$ is a constant value, $A_f$ and $A_s$ are fractions of fast and slow recovering components, while $\tau_f$ and $\tau_s$ are the time constants of fast and slow recovering components, respectively.

Results are presented as means ± standard error, and statistical comparisons were made using the unpaired Student's $t$-test to evaluate the difference between means. Statistical significance was assumed for $P < 0.05$. All the experiments were done at room temperature (20–22°C).

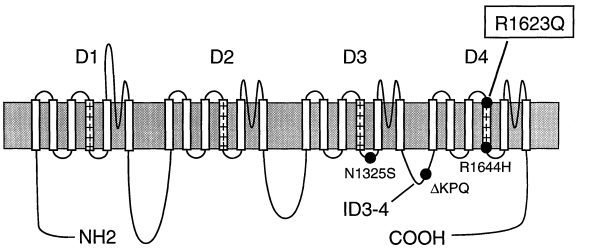


Fig. 1. Schematic representation of the predicted transmembrane topology of human cardiac $Na^+$ channel α subunit (hH1) and the location of LQT3 mutations.

## 3. Results

### 3.1. Macroscopic $Na^+$ current

Fig. 2A shows representative TTX-sensitive $Na^+$ currents recorded during a 50 ms test depolarization to −20 mV from a holding potential of −120 mV. Small persistent TTX-sensitive currents (less than 5% of the peak current) were not observed in WT but were evident in R1623Q during depolarizations, a commonly observed feature in previously studied LQT3 mutations (ΔKPQ, N1325S, and R1644H) [8,9]. One of the biophysical characteristics that distinguishes R1623Q from other LQT3 mutations is the slow macroscopic inactivation. Macroscopic currents of either WT or R1623Q decayed with a biexponential time course. The time constant ($\tau_h$) values of both fast ($\tau_f$) and slow ($\tau_s$) components of R1623Q at −20 mV were significantly larger than those of WT (WT: $\tau_f = 0.58 \pm 0.04$ ms, $\tau_s = 4.45 \pm 0.18$ ms, $n = 16$; R1623Q: $\tau_f = 1.88 \pm 0.26$ ms, $\tau_s = 8.30 \pm 1.25$ ms, $n = 14$; $P < 0.01$). By

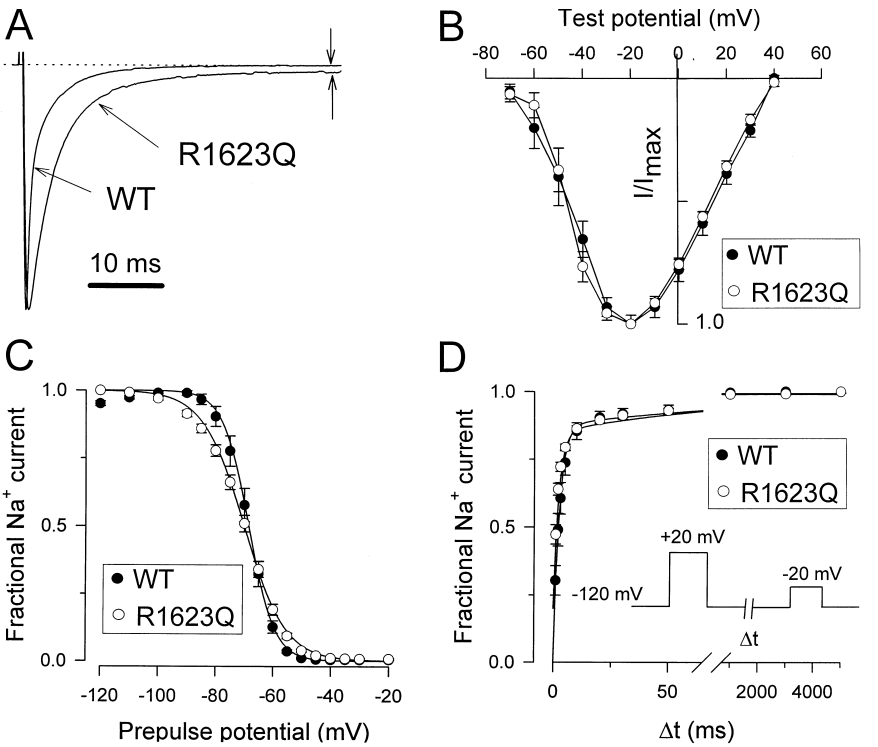


Fig. 2. Two-electrode voltage-clamp recordings made in *Xenopus* oocytes expressing either WT or R1623Q $Na^+$ channel α subunits. A: TTX-sensitive $Na^+$ currents recorded in *Xenopus* oocytes expressing either WT or R1623Q-hH1. $Na^+$ currents were recorded in the presence or absence of 30 μM TTX during a 50 ms test depolarization to −20 mV from a holding potential of −120 mV. TTX-sensitive currents were obtained by subtracting currents in the absence from those in the presence of TTX as reported earlier [8]. Peak amplitudes of the TTX-sensitive currents of both WT and R1623Q $Na^+$ channels were scaled and superimposed to illustrate differences in the time course of current decay. Sodium current expression was similar in WT and R1623Q RNA-injected oocytes. Time calibration bar represents 10 ms. Vertical arrows indicate the amplitude of TTX-sensitive persistent current observed in R1623Q. B: Normalized current-voltage relationships for the peak currents for WT (closed circles) and R1623Q (open circles). C: Steady-state inactivation. Steady-state inactivation was assessed by stepping the membrane potential to a voltage between −120 mV and −20 mV for 500 ms, and then peak $Na^+$ current was measured during a −20 mV test potential. Currents were normalized to values obtained with a prepulse of −120 mV for WT (closed circles) and R1623Q (open circles). The midpoint voltage ($V_{1/2}$) and the slope factor ($k$) of the $h_\infty$ curve for WT are $-68.7 \pm 1.3$ mV and $4.0 \pm 0.18$; for R1623Q these values are $-70.1 \pm 0.90$ mV and $7.0 \pm 0.16$, respectively. D: Recovery from inactivation. Recovery from inactivation was assessed by a double pulse protocol consisting of a 500 ms prepulse to +20 mV designed to fully inactivate both WT (closed circles) and R1623Q (open circles), followed by a variable duration pulse to −120 mV and a test potential to −20 mV. The fractional current amplitude was determined by as the ratio of peak currents measured at −20 mV after a given test interval ($\Delta t$) to the maximum current amplitude. The pulse protocol cycle time was 10 s.

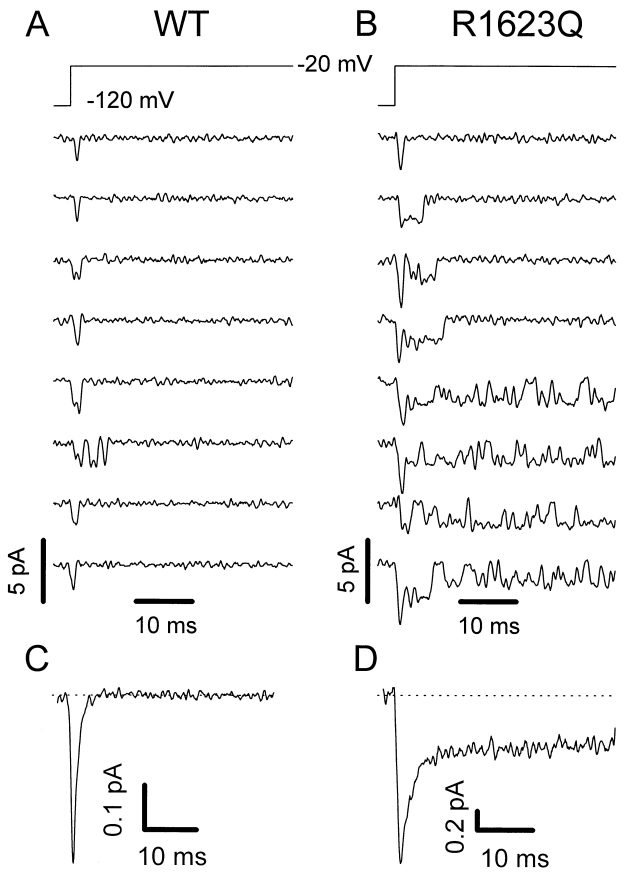


Fig. 3. Single channel recordings of $Na^+$ channels in inside-out membrane patches excised from *Xenopus* oocytes. Recordings were made during 40 ms duration voltage-clamp steps to −20 mV from a holding potential of −120 mV. A: Representative recordings from WT $Na^+$ channel currents. B: Representative recordings from R1623Q $Na^+$ channel currents. Mutant channels occasionally entered a non-inactivating bursting mode (lower four sweeps) from a normal inactivating mode (upper four sweeps). Scaled ensemble averages of 540 traces of WT channel (C) and 392 traces of R1623Q mutant channel (D). The peak amplitudes were scaled to illustrate differences in the inactivation time courses. Similar results were obtained in replicate experiments for each channel. Horizontal bars indicate 10 ms, and the vertical bar indicates the current amplitude as shown.

contrast, scaled current-voltage plots of peak currents of WT and R1623Q were nearly superimposable (Fig. 2B), and the time to peak value of each channel was comparable (WT: $1.1 \pm 0.1$ ms, $n = 9$; R1623Q: $1.1 \pm 0.1$ ms, $n = 8$), suggesting that the activation kinetics were minimally affected in R1623Q. The midpoint of steady-state inactivation ($V_{1/2}$) was not altered in the mutant (WT: $-68.7 \pm 1.3$ mV, $n = 11$; R1623Q: $-70.1 \pm 0.90$ mV, $n = 13$; $P > 0.1$), however, the slope factor was significantly larger in R1623Q (WT: $k = 4.0 \pm 0.18$, $n = 11$; R1623Q: $k = 7.0 \pm 0.16$, $n = 13$; $P < 0.001$), indicating that steady-state inactivation was less voltage-sensitive in R1623Q than in WT (Fig. 2C). The time courses of recovery from inactivation of WT and R1623Q were nearly superimposable (Fig. 2D). The time constants of fast and slow recovering components of each channel were: WT: $\tau_f = 3.0 \pm 0.34$ ms, $\tau_s = 103 \pm 23$ ms, $n = 14$; R1623Q: $\tau_f = 2.3 \pm 0.14$ ms, $\tau_s = 82 \pm 13$ ms, $n = 17$ (no significant differences).

### 3.2. Patch-clamp recordings

To understand the precise pathophysiological mechanisms responsible for the R1623Q dysfunction, we performed single channel analysis on both WT and R1623Q. Fig. 3 shows representative single channel currents elicited by 40 ms depolarizations to −20 mV for WT (A) and R1623Q (B). Ensemble average current shows rapid inactivation without late current during depolarization in the WT (C), however, R1623Q (D) showed significantly slow inactivation followed by persistent inward current. These results are consistent with the observations in two-electrode voltage-clamp recordings (Fig. 2A). The single channel conductance of R1623Q channel was $22 \pm 1$ pS ($n = 4$), which was comparable to WT [18]. The kinetics of channel opening and closing of R1623Q were clearly altered as compared to those of WT. Mean open times were increased in the patches of R1623Q ($\tau = 1.7 \pm 0.1$ ms, $n = 7$) as compared with WT ($\tau = 0.6$ ms) (Fig. 4), whereas LQT3 mutant ΔKPQ has near normal mean open time ($\tau = 0.6$ ms) [8]. R1623Q also exhibited a greater tendency for bursting than WT (Fig. 3A,B), however, the mean open times of initial opening and burst opening of R1623Q were identical ($\tau = 1.7$ ms). These results suggest that the inactivation rate from the open state is decreased in the R1623Q mutant channels [19], and this represents a distinct biophysical mechanism underlying the R1623Q mutation.

## 4. Discussion

This study demonstrates the functional properties of the novel de novo LQT3 mutation R1623Q. Electrophysiological abnormalities of this mutant $Na^+$ channel were observed mainly in its inactivation but not in activation properties. The R1623Q mutant differs substantially from other previously studied LQT3 mutations in the presence of significantly slower macroscopic inactivation. The other three LQT3 mutations exhibit similar biophysical abnormalities characterized by near normal macroscopic inactivation and activation, but small persistent currents were evident during long depolarizations (less than 4% of peak current) [8,9]. Single channel analyses have demonstrated that the mean open time of ΔKPQ was compatible with WT [8]. It is speculated that the mutant channel fluctuates between a normal gating mode and a non-inactivating mode (modal gating) [8] thereby generating persistent inward current, which in turn prolongs ventricular repolarization. Biophysical behaviors of the other two point mutations (N1325S, and R1644H) are qualitatively similar to ΔKPQ [9,20]. By contrast, the slower macroscopic inactivation rates of the R1623Q mutant channel cannot be explained solely by the modal gating theory.

The slower inactivation rate observed for R1623Q may be the consequence of the following at the single channel level: (1) an increase in the duration of opening, and/or (2) an increase in the number of openings during a depolarization [19,21]. These mechanisms could be due to a defect in the process of inactivation. At the single channel level, R1623Q exhibited both a normal gating mode and a non-inactivating burst mode. Furthermore, the mean open time of R1623Q ($\tau = 1.7$ ms) was approximately three times longer than WT ($\tau = 0.6$ ms) as well as LQT3 mutant ΔKPQ ($\tau = 0.6$ ms) [8]. To explain the observations from whole cell and single channel experiments, we speculate that two biophysical mechanisms, modal gating and prolongation of mean open time, are in-

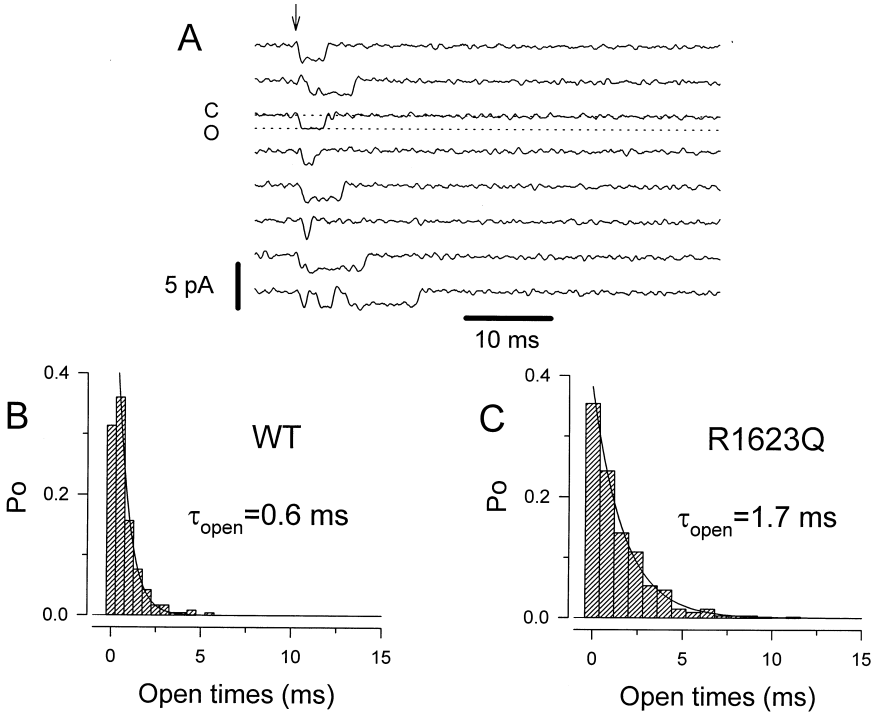


Fig. 4. Open time distributions of WT and R1623Q. Unitary current was estimated from all points, amplitude histograms and open times were measured using a 50% threshold-crossing criterion as described [31]. Mean open times were measured from patches expressing single channels. A: Representative recordings of a patch expressing a single channel of R1623Q. Open time distributions were made by sorting open distributions into bins (WT: 0.5 ms, R1623Q: 0.8 ms) and plotting (or fitting) the numbers of openings per bin as a function of open time for WT (B) and R1623Q (C). Horizontal and vertical bars indicate 10 ms and 5 pA, respectively.

volved in the pathogenesis of LQT3 associated with the R1623Q mutation.

Considerable observations are available now for the functional disturbances of naturally occurring mutations of hereditary muscle disorders. Arginine-1623 in hH1 corresponds to the arginine-1448 (R1448) in the human skeletal muscle $Na^+$ channel $\alpha$ subunit (hSkM1). Two missense mutations (R1448H, R1448C) of this residue have been identified in patients with paramyotonia congenita patients [22]. These mutations exhibit profound abnormalities in inactivation [23,24]. These characteristics are similar to those of R1623Q in our study. Such severe inactivation defects in skeletal muscle $Na^+$ channels lead to sarcolemmal hyperexcitability and the clinical phenotype of myotonia. Although similar abnormalities in cardiac $Na^+$ channels were originally thought to be incompatible with life [9], the severe biophysical characteristics of R1623Q correlate well with the clinical phenotype. The patient developed a potentially lethal ventricular arrhythmia, torsades de pointes, at 35 days after birth, and has been successfully treated with the $Na^+$ channel blocker mexilletine. Based on these observations, we propose that R1623Q is associated with an essentially severe LQT3 subtype and has biophysical characteristics distinct from those of the three previously studied LQT3 mutations [8–10].

Voltage-dependent activation and inactivation are two crucial functional features of $Na^+$ channels [25]. Considerable efforts have been made to map the regions involved in these functions. It is generally accepted that the positively charged S4 helices move across the electrical field in response to depolarization and function as voltage sensors to open the activation gates [26,27]. There is also strong evidence suggesting an essential role for the cytoplasmic linker region connecting domain 3 and domain 4 (ID3, 4) in fast inactivation [26,28–30]. The LQT3 mutations R1623Q and R1644H as well as paramyotonia congenita mutations R1448H/C are localized in S4 segment of domain 4 (S4/D4) of $Na^+$ channels, and their functional disturbances are mainly in inactivation but not in activation. The precise mechanism of impaired inactivation of the R1623Q mutation may be a functional defect in activation-inactivation coupling of the $Na^+$ channel that has been previously demonstrated in paramyotonia congenita mutations R1448H/C [23].

*Acknowledgements:* This study was supported in part by the Eimatsu Takakuwa Research Award and The Akiyama Foundation Prize for N.M.

## References

[1] Curran, M.E., Splawski, I., Timothy, K.W., Vincent, G.M., Green, E.D. and Keating, M.T. (1995) Cell 80, 795–803.
[2] Wang, Q., Shen, J., Splawski, I., Atkinson, D., Li, Z., Robinson, J.L., Moss, A.J., Towbin, J.A. and Keating, M.T. (1995) Cell 80, 805–811.
[3] Schott, J.J., Charpentier, F., Peltier, S., Foley, P., Drouin, E., Bouhour, J.B., Donnelly, P., Vergnaud, G., Bachner, L., Moisan, J.P., Le Marec, H. and Pascal, O. (1995) Am. J. Hum. Genet. 57, 1114–1122.
[4] Wang, Q., Curran, M.E., Splawski, I., Burn, T.C., Millholland, J.M., VanRaay, T.J., Shen, J., Timothy, K.W., Vincent, G.M., de Jager, T., Schwartz, P.J., Toubin, J.A., Moss, A.J., Atkinson, D.L., Landes, G.M., Connors, T.D. and Keating, M.T. (1996) Nature Genet. 12, 17–23.
[5] Splawski, I., Tristani-Firouzi, M., Lehmann, M.H., Sanguinetti, M.C. and Keating, M.T. (1997) Nature Genet. 17, 338–340.
[6] George Jr., A.L., Varkony, T.A., Drabkin, H.A., Han, J., Knops, J.F., Finley, W.H., Brown, G.B., Ward, D.C. and Haas, M. (1995) Cytogenet. Cell Genet. 68, 67–70.

[7] Wang, Q., Shen, J., Li, Z., Timothy, K., Vincent, G.M., Priori, S.G., Schwartz, P.J. and Keating, M.T. (1995) Hum. Mol. Genet. 4, 1603–1607.
[8] Bennett, P.B., Yazawa, K., Makita, N. and George Jr., A.L. (1995) Nature 376, 683–685.
[9] Wang, D.W., Yazawa, K., George Jr., A.L. and Bennett, P.B. (1996) Proc. Natl. Acad. Sci. USA 93, 13200–13205.
[10] Wang, D.W., Yazawa, K., Makita, N., George Jr., A.L. and Bennett, P.B. (1997) J. Clin. Invest. 99, 1714–1720.
[11] Yamagishi, H., Furutani, M., Kamisago, M., Moriwaka, Y., Kojima, Y., Hino, Y., Furutani, Y., Kimura, M., Imamura, S., Takao, A., Momma, K. and Matsuoka, R. (1997) Hum. Mutat. (Mutation in Brief #140 Online (http://journals.wiley.com/1059-7794/humuann.htm).
[12] Higuchi, R. (1990) in: PCR protocols (Innis, M.A., Gelfand, D.H. and Sninsky, J.J., Eds.), pp. 177–183, Academic Press, San Diego, CA.
[13] Krieg, P.A. and Melton, D.A. (1987) Methods Enzymol. 155, 397–415.
[14] Makita, N., Bennett Jr., P.B. and George Jr., A.L. (1996) Circ. Res. 78, 244–252.
[15] Makita, N., Bennett, P.B. and George, A.L. (1996) J. Neurosci. 16, 7117–7127.
[16] Schreibmayer, W., Lester, H.A. and Dascal, N. (1994) Pflügers Arch. 426, 453–458.
[17] Bennett, P.B., Valenzuela, C., Chen, L.Q. and Kallen, R.G. (1995) Circ. Res. 77, 584–592.
[18] Fozzard, H.A. and Hanck, D.A. (1996) Physiol. Rev. 76, 887–926.
[19] Vandenberg, C.A. and Horn, R. (1984) J. Gen. Physiol. 84, 535–564.
[20] Dumaine, R., Wang, Q., Keating, M.T., Hartmann, H.A., Schwartz, P.J., Brown, A.M. and Kirsch, G.E. (1996) Circ. Res. 78, 916–924.
[21] Aldrich, R.W., Corey, D.P. and Stevens, C.F. (1983) Nature 306, 436–441.
[22] Ptácek, L.J., George Jr., A.L., Barchi, R.L., Griggs, R.C., Riggs, J.E., Robertson, M. and Leppert, M.F. (1992) Neuron 8, 891–897.
[23] Chahine, M., George Jr., A.L., Zhou, M., Ji, S., Sun, W., Barchi, R.L. and Horn, R. (1994) Neuron 12, 281–294.
[24] Yang, N., Ji, S., Zhou, M., Ptácek, L.J., Barchi, R.L., Horn, R. and George Jr., A.L. (1994) Proc. Natl. Acad. Sci. USA 91, 12785–12789.
[25] Catterall, W.A. (1995) Annu. Rev. Biochem. 64, 493–531.
[26] Stühmer, W., Conti, F., Suzuki, H., Wang, X.D., Noda, M., Yahagi, N., Kubo, H. and Numa, S. (1989) Nature 339, 597–603.
[27] Yang, N., George Jr., A.L. and Horn, R. (1996) Neuron 16, 113–122.
[28] Vassilev, P., Scheuer, T. and Catterall, W.A. (1989) Proc. Natl. Acad. Sci. USA 86, 8147–8151.
[29] West, J.W., Patton, D.E., Scheuer, T., Wang, Y., Goldin, A.L. and Catterall, W.A. (1992) Proc. Natl. Acad. Sci. USA 89, 10910–10914.
[30] Patton, D.E., West, J.W., Catterall, W.A. and Goldin, A.L. (1992) Proc. Natl. Acad. Sci. USA 89, 10905–10909.
[31] Valenzuela, C. and Bennett Jr., P.B. (1994) Biophys. J. 67, 161–171.